Wearer-Prosthesis Interaction for Symmetrical Gait: A Study Enabled by Reinforcement Learning Prosthesis Control

Yue Wen, Minhan Li, Jennie Si, *Fellow, IEEE,* and He(Helen) Huang, *Senior Member, IEEE*

***Abstract*—With advances in robotic prostheses, researchers attempt to improve amputee's gait performance (e.g., gait symmetry) beyond restoring normative knee kinematics/kinetics. Yet, little is known about how the prosthesis mechanics/control influence wearer-prosthesis' gait performance, such as gait symmetry, stability, etc. This study aimed to investigate the influence of robotic transfemoral prosthesis mechanics on human wearers' gait symmetry. The investigation was enabled by our previously designed reinforcement learning (RL) supplementary control, which simultaneously tuned 12 control parameters that determined the prosthesis mechanics throughout a gait cycle. The RL control design facilitated safe explorations of prosthesis mechanics with the human in the loop. Subjects were recruited and walked with a robotic transfemoral prosthesis on a treadmill while the RL controller tuned the control parameters. Stance time symmetry, step length symmetry, and bilateral anteroposterior (AP) impulses were measured. The data analysis showed that changes in robotic knee mechanics led to movement variations in both lower limbs and therefore gait temporal-spatial symmetry measures. Consistent across all the subjects, inter-limb AP impulse measurements explained gait symmetry: the stance time symmetry was significantly correlated with the net inter-limb AP impulse, and the step length symmetry was significantly correlated with braking and propulsive impulse symmetry. The results suggest that it is possible to personalize transfemoral prosthesis control for improved temporal-spatial gait symmetry. However, adjusting prosthesis mechanics alone was insufficient to maximize the gait symmetry. Rather, achieving gait symmetry may require coordination between the wearer's motor control of the intact limb and adaptive control of the prosthetic joints. The results also indicated that the RL-based prosthesis tuning system was a potential tool for studying wearer-prosthesis interactions.**

***Index Terms*—Wearer-prosthesis interaction, robotic knee prosthesis, reinforcement learning, gait asymmetry, anteroposterior impulse**

I. Introduction

To restore locomotion for people with transfemoral amputations, research efforts in the last decades have been devoted to the design and control of robotic prostheses [1]–[10] that mimic biological knee (and ankle) function. These advanced robotic knee prostheses enable transfemoral amputees to negotiate uneven terrains (such as stairs and ramps) with normative patterns [9]–[13], reduce asymmetry in muscle activation [14] or temporal-spatial gait symmetry [15], [16], and perform non-rhythmic tasks (e.g., backward walking) [16]. However, all these benefits rely on fine-tuned and personalized control settings [9]–[11], [13]–[16]. Currently, robotic knee prostheses are either manually tuned by clinicians [1], [17] or automatically tuned by intelligent controllers [18], [19] in order to generate normative knee kinematics, which has been widely used as the goal or evaluation criterion of powered knee prosthesis control [2], [5]. However, the robotic prosthesis wearer's gait performance (e.g., gait symmetry, stability, and energy expenditure) has not consistently improved [7]–[11]. In order to improve the gait of prosthesis wearers beyond knee kinematics through prostheses tuning, it is critical to understand the physical wearer-prosthesis interaction, including how the mechanics of prostheses influence human wearers' movement and dynamics in locomotion.

To date, there are only a handful of studies about the influence of robotic prosthesis control/mechanics on gait performance [20], [21]. Among these, most focus on a robotic ankle device, studying one control variable such as push-off timing [20] or push-off power [21] in one gait phase at a time; and they use metabolic cost as the main performance outcome. Another study investigated the effect of a control gain on the kinematics/kinetics symmetry of ankle prostheses [22]. These studies are inadequate to understand how complex robotic knee mechanics, which are usually determined by 12 or more parameters during an entire gait cycle [1], [2], [5], [23], affects the prosthesis wearer's gait. Additionally, although metabolic cost is an important metric for gait evaluation, other gait metrics, such as symmetry, are equally critical in amputee clinics. For example, temporal-spatial gait symmetry is one of the common gait evaluation metrics for lower limb amputees [24]. It reveals the fundamental timing and position information of a person's gait [25]. Asymmetrical gait is frequently reported in people with unilateral lower limb amputation [26]–[29], and is associated with many secondary issues, such as osteoarthritis of unamputated joints [30] and lower back pain [31]. Theoretically, reduction of push-off impulse/work (namely propulsive impulse or work) from one leg leads to gait temporal-spatial asymmetry [27], [32]. Many experimental studies on pathological gait have shown evidence to support this mechanism [32], [33], including cases of amputees walking with energetically passive prostheses due to inadequate push-off impulse from prosthetic limb [28], [29]. However, when walking with robotic prostheses, which are capable of

This work was partly supported by National Science Foundation #1563454, #1563921, #1808752, #1808898, and NIH EB024570.

Y. Wen, M. Li, and H. Huang are with the UNC & NC State Joint Department of Biomedical Engineering, NC State University, Raleigh, NC, 27695-7115; University of North Carolina at Chapel Hill, Chapel Hill, NC 27599 USA.

J. Si is with the Department of Electrical, Computer, and Energy Engineering, Arizona State University, Tempe, AZ, 85281 USA.

Corresponding author: He(Helen) Huang (hhuang11@ncsu.edu).

providing positive work at prosthetic joints for increased push-off force, gait asymmetry persists [19]. The open questions are whether and how the mechanics of the robotic prosthesis influence the wearer-prosthesis gait performance reflected by impulses and gait symmetry.

Addressing these open questions is inherently challenging partly because there lacks a practical method to safely explore high-dimensional prosthesis control. Usually, robotic knee prostheses use a finite-state machine (FSM) to adjust the impedance of prosthetic joints in each gait phase (defined as the state in FSM) [2], [5], [23], [34]. Therefore, the mechanics of a robotic knee prosthesis are determined by 12 or more individual control parameters [1], [2], [23]. In order to study wearer-prosthesis interactions, a method that can facilitate the safe and practical exploration of high-dimensional prosthesis control with the human in the loop is necessary. Manual exploration by a clinician is inefficient and impractical since there are too many control parameters. Linearly scanning through the control parameter spaces can be unsafe and inefficient because we do not know the safe control parameter spaces, and the combinations of the control parameters are tremendous and redundant [35].

Reinforcement learning (RL) based prosthesis tuning [18] is a natural candidate to address the aforementioned challenge. The RL tuning system was previously designed to personalize prosthesis control. It adjusted the mechanics of the robotic knee prosthesis through changing the 12 impedance parameters simultaneously in order to achieve the desired knee movement pattern in walking. It can be readily applied as a practical and safe method to study the effects of high-dimensional prosthesis control on the wearer's gait. First, our RL algorithm is within a basic actor-critic framework where the actor produces control actions and the critic provides evaluations of the control action [36]. Here, we used neural networks to represent/approximate the control actions and the cost function which evaluates how effective the actions are. As such, our design approach is scalable to high-dimensional control inputs and it could introduce opportunities for exploration: some actions may result in an increase in the cost value but as learning progresses, the approximated cost value is minimized to provide optimal control. This is unlike those search algorithms [38], [39] that only explore the parameters for improving gait response monotonically. Our RL approach allows probing parameters in non-deterministic directions which resulted in better or worse performance. Second, we have shown that RL can sample a limited number of parameter combinations to approximate the value function and the control policy [18], [40]. Finally, the RL tuner by design ensures a human-like locomotion pattern and the wearer's upright walking stability and safety by maintaining the basic knee kinematic pattern and allowing variations of knee motion within a range [18].

Empowered by the RL prosthesis control, the goal of this study is to investigate the influence of changes in the mechanics (the impedance control) of the robotic knee prosthesis on the inter-limb impulses and gait temporal-spatial symmetry. We quantified 1) the influence of the robotic prosthesis mechanics on ground reaction force/impulse, and gait temporal-spatial symmetry, and 2) the relationship between the inter-limb impulses and temporal-spatial gait symmetry. To our best knowledge, limited studies have been conducted to investigate the influence of robotic knee prosthesis mechanics on the human wearer's gait symmetry. The study will contribute to important knowledge in wearer-robot interactions and guide the future design and control of robotic knee prostheses for symmetrical gait.

II. Methods

A. Wearer-prosthesis system

1) Experimental knee prosthesis: The robotic knee prosthesis used in this study was equipped with a motor, an angle sensor at the rotating knee joint, and a load cell in the pylon [23]. The robotic knee prosthesis was controlled by a commonly-used finite-state machine impedance controller [2], [34]. The finite-state machine cyclically transitioned through four finite states corresponding to four gait phases of one gait cycle: stance flexion, stance extension, swing flexion, and swing extension. Within each finite state, the prosthetic knee joint torque τ was regulated by an impedance controller (Eq. 1), which depends on three impedance parameters (i.e. equilibrium position θ_e, stiffness coefficient k, damping coefficient b), and two real-time measurements from the prosthetic knee joint (angle θ, angular velocity ω).

$$\tau_m = k_m(\theta - \theta_{em}) + b_m\omega \tag{1}$$

where subscript m is the phase index ($m = 1, 2, 3, 4$). Therefore, the mechanics of the robotic knee prosthesis were determined by a total of 12 impedance parameters.

2) Knee kinematics: Typically, the knee joint angle trajectory in one gait cycle has a local maximum during stance flexion and swing flexion, and a local minimum during stance extension and swing extension (Fig. 1). Therefore, we represented the knee kinematics in one gait cycle with four pairs of peak angle values P and their respective duration values D: $[P_m, D_m]$, where $m = 1, 2, 3, 4$. Similarly, we extracted the same features from normative knee kinematics as target features, denoted as $[\bar{P}_m, \bar{D}_m]$.

3) Tuning/exploration process: The impedance parameter tuning process included parameter updates and human-prosthesis evaluation. For the ease of discussion without causing any confusion, we drop the phase index m hereon.

At iteration n, the impedance parameters were denoted by

$$\begin{aligned} I(n) &= I(n-1) + \Delta I(n-1) \\ &= [k(n), \theta_e(n), b(n)]^T, \end{aligned} \tag{2}$$

where $\Delta I(n-1)$ denote the adjustments to the impedance parameters by auto-tuner.

The states of the wearer-prosthesis system were defined as

$$X(n) = \gamma \odot [x^T(n) - \bar{x}^T, x^T(n) - x^T(n-1)]^T, \tag{3}$$

where x are the measured features $[P, D]$, $\bar{x}$ are the target features $[\bar{P}, \bar{D}]^T$, and $\gamma \in \mathbb{R}^{4\times 1}$ is a vector of scaling factors to normalize the states to $[-1, 1]$. $\odot$ is the Hadamard product, which is an element-wise multiplication of two vectors with the same dimension.

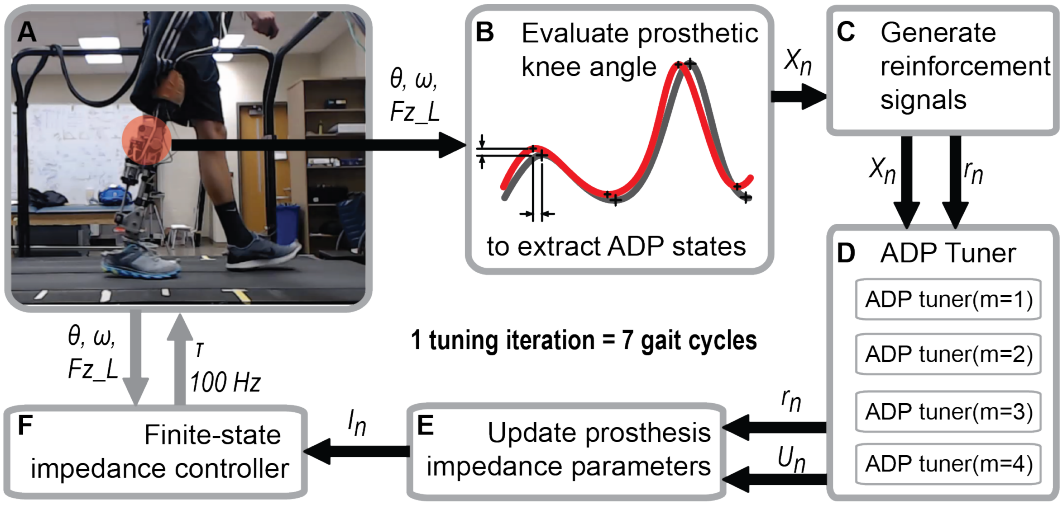

Fig. 1. Framework of the human-in-the-loop automatic impedance parameter tuning by reinforcement learning control (auto-tuner). (A and F) The wearer-prosthesis system, where the torque τ of the robotic knee prosthesis is regulated by the finite-state machine impedance controller. (B) Evaluation module, the bridge between the wearer-prosthesis system and RL auto-tuner, which takes in measurements from the robotic prosthesis (joint angle θ, angular velocity ω, and vGRF Fz_L) and generates the RL state X_n. (C) Generate RL reinforcement signal r_n from the wearer-prosthesis system according to [18]. (D) RL auto-tuner, which consists of 4 blocks, implemented with direct heuristic dynamic programming (dHDP) [36], [37], corresponding to the prosthesis controllers in four gait phases. (E) Update the impedance parameters to get I_n with the auto-tuner outputs U_n and reinforcement signal r_n. The subscript n represents the iteration index.

B. Reinforcement learning based auto-tuner

We applied an RL-based auto-tuner to explore the impedance parameter space of a robotic knee prosthesis control while ensuring the safety of the wearer-prosthesis system. The auto-tuner was implemented using the direct heuristic dynamic programming (dHDP) (Fig. 1), as used in [18], [40]. The auto-tuner adjusted the three impedance parameters in each phase iteratively to minimize accumulated future error based on the two features of the corresponding gait phase. Each auto-tuner block was implemented using direct heuristic dynamic programming (dHDP) [36], [37], which consisted of an action neural network (ANN) and a critic neural network (CNN). With our previously demonstrated successes of applying dHDP to solving optimal learning control problems such as the stabilization, tracking, and reconfiguration control of Apache helicopters [41]–[43], and oscillation damping in a large power system [44], dHDP is readily applicable to impedance parameter tuning to enable safe walking of a human wearing a robotic prosthesis knee device.

The ANN represented the impedance parameter control policy which mapped the states of the wearer-prosthesis system (X) to action (U) which was the adjustment to the impedance parameter of the robotic knee prosthesis. Specifically,

$$U(n) = \varphi(W_{a2}(n)\varphi(W_{a1}(n)X(n))), \tag{4}$$

where $W_{a1} \in \mathbb{R}^{7\times4}$ and $W_{a2} \in \mathbb{R}^{3\times7}$ were the ANN weight matrices, and $\varphi(\cdot)$ was the activation function. The adjustments of impedance parameters were calculated according to

$$\Delta I(n) = \beta \odot U(n), \tag{5}$$

where $\beta \in \mathbb{R}^{3\times1}$ represents scaling factors to assign physical magnitudes to the actions.

The CNN approximated the discounted total cost-to-go as an evaluation function of the performance of the human-prosthesis system and the decisions from the ANN.

$$\hat{J}(n) = W_{c2}(n)\varphi(W_{c1}(n)[X^T(n), U^T(n)]^T), \tag{6}$$

where $W_{c1} \in \mathbb{R}^{7\times7}$ and $W_{c2} \in \mathbb{R}^{1\times7}$ are the weight matrices, and X and U are the state input and action output of the ANN.

In this study, the primary reinforcement signal r, or the stage cost, of the wearer-prosthesis system was the same as those in [18] where safety bounds were taken into account in order to ensure wearer-prosthesis system upright stability. The total cost-to-go was then defined as

$$\begin{aligned} J(n) &= r(n+1) + \alpha r(n+2) + ... \\ &= r(n+1) + \alpha J(n+1), \end{aligned} \tag{7}$$

where α is a discount rate ($0 < \alpha < 1$).

The CNN weights were updated so that the following Bellman equation was optimized, the solution of which was an optimal estimate of the total cost-to-go.

$$E_c(n) = \frac{1}{2}(\alpha\hat{J}(n) - (\hat{J}(n-1) - r(n)))^2. \tag{8}$$

The ANN weights were updated in order for the total cost-to-go to reach an ultimate goal level, i.e.,

$$\begin{aligned} E_a(n) &= \frac{1}{2}(\hat{J}(n) - \bar{J})^2 \\ &= \frac{1}{2}(\hat{J}(n))^2, \end{aligned} \tag{9}$$

where $\bar{J}$ was the desired ultimate objective and was 0 corresponding to "success". A detailed weight update algorithm can be found in [40].

For each tuning iteration, the RL auto-tuner followed four steps: 1) collected state inputs from the wearer-prosthesis system as the sample mean of the previous 7 gait cycles, 2)

updated CNN and ANN based on the reinforcement signal, 3) updated the impedance parameters according to Eq. 4, and Eq. 5, and 4) allowed the subject to walk with the new impedance parameters for 7 gait cycles. After each tuning iteration, the RL auto-tuner updated any combination of the 12 total impedance parameters across the 4 blocks.

C. Experimental protocol

With IRB approval and signed consent, six subjects (3 able-bodied subjects and 3 transfemoral amputees; Table I) walked on an instrumented treadmill with an experimental knee prosthesis while reinforcement learning tuned the control parameters (Fig. 1). Amputee subjects wore their daily socket and were fitted with the experimental powered knee prosthesis by a prosthetist. Able-bodied subjects wore a L-shape adapter to walk with the powered knee prosthesis. All subjects were trained to walk with the powered knee prosthesis on a treadmill at a speed of 0.6 m/s for more than six sessions, until they felt comfortable and confident enough to walk with the experimental prosthesis without holding the handrail.

We conducted this study with each subject over four experimental sessions, each session beginning with a different and naïve RL auto-tuner (i.e., randomly initialized knowledge or network weights) and a different initial impedance parameter set for the robotic knee prosthesis. The initial impedance parameter sets were randomly selected from a database of prosthesis control parameter sets, applied in our previous study and validated to meet three criteria: 1) the subject was subjectively able to walk without severe difficulty as visually observed by the researcher (e.g., tight grip on the handrails) or verbally expressed by the subject, 2) the root-mean-square error of the prosthetic knee joint kinematics with respect to the normative knee kinematics was greater than 4 degrees (i.e., the initial impedance parameter set did not generate the normative knee kinematics), and 3) the features of the prosthetic knee joint kinematics were within the allowed safety ranges [18].

Once we selected an appropriate initial impedance parameter set, we used the RL auto-tuner to tune the impedance parameters over multiple 3-minute trials with 3-minute breaks between each trial to prevent fatigue from confounding our results. At the start of each trial, the subject walked for 30 seconds to acclimate to the testing environment. We then activated the RL auto-tuner, which evaluated the prosthetic knee kinematics performance and updated the impedance parameters every 7 strides for 2.5 minutes. The 7-stride per iteration setting was to attenuate the effects of stride-to-stride variance in walking. We did not observe adaptation with moderate parameter changes in the pilot study. We terminated the tuning procedure if either of 2 criteria was met: 1) the tuning iteration numbers reached 70 iterations (in order to prevent subject fatigue); 2) the feature errors of prosthetic knee kinematics remained in the tolerance range for 3 of the previous 5 tuning iterations.

Prosthetic knee joint angle was recorded through the angle sensor on the prosthetic joint and the ground reaction forces were recorded through the instrumented treadmill (1000 Hz; Bertec Corp., Columbus, OH, USA) during the experiments. Spatial gait performance metrics used data from two markers on each calcaneus, which were recorded by an 8-camera motion caption system (100 Hz; VICON, Oxford, UK).

D. Data processing and analysis

1) Preprocessing: All kinematics and ground reaction force data were segmented and aligned for each tuning iteration, which included 7 gait cycles during which the prosthetic knee was controlled by the same impedance parameters. We filtered the ground reaction force data and knee kinematics using a low-pass filter with a cutoff frequency of $20Hz$. Then we identified the gait events (heel strike and toe off) using vertical ground reaction force with an threshold of $30N$. With the gait events, we calculated the features of knee kinematics, stance time symmetry index, and step length symmetry index. Additionally, we normalized the ground reaction forces with each subject's body weight and calculated the ground reaction force impulses.

2) Spatial-temporal parameters: Stance time of each leg was calculated with the heel strike and toe off events of the same leg. The step length of each leg was measured by the anteroposterior distance between two calcaneus markers at the corresponding heel strike.

For both variables, a symmetry index (SI) was calculated to quantify asymmetries between the prosthetic leg and the intact leg:

$$SI_V = \frac{V_i - V_p}{1/2(V_i + V_p)} \tag{10}$$

where V_i is the stance time or step length measurement from the intact limb, and V_p is the respective measurement from the prosthetic limb. SI was negative when a measurement from the prosthetic side was greater than that from the intact side.

3) Impulse: To capture the dynamic interaction between the wearer-prosthesis system and the environment, we calculated the braking and propulsive impulses for each leg based on the method from [45]. The braking and propulsive impulses of each leg were defined as the time integral of the positive and negative range of the anteroposterior ground reaction of each leg.

The method for computing the impulses based on that of [45] was implemented as follows. To account for variations in the ground reaction force by the prosthesis wearers, we divided the stance phase into three time bins: 1) initial double limb support (IDS), 2) single limb stance (SS), 3) terminal double limb support (TDS). Accordingly, we computed the impulses generated during each respective time period in a gait cycle. The ground reaction force during single limb stance was separated into two portions: integration of the negative portion as braking impulse and integration of the positive portion as propulsive impulse. The braking impulse was calculated by adding the integration of ground reaction force during initial double limb support and that of the negative portion of ground reaction force during single limb stance. The propulsive impulse was calculated by adding the integration of ground reaction force during terminal double limb support and that of the positive portion of ground reaction force during single limb stance. Specifically,

TABLE I
SUBJECT INFORMATION

Subject	Gender	Body weigh	Height	Age	Since amputation	Amputated side	Prescribed device	Cause of amputation
TF1	Male	66 kg	1.83 m	21 years	6 years	Right	Ottobock Genium	Cancer
TF2	Male	91 kg	1.80 m	58 years	46 years	Left	Ottobock C-Leg	Cancer
TF3	Male	95 kg	1.88 m	30 years	30 years	Left	Freedom Innovations Plié 2	Congenital
AB 1-3	Male	68 $\pm$ 5 kg	1.78 $\pm$ 0.01 m	33 $\pm$ 8 years	N/A	N/A	N/A	N/A

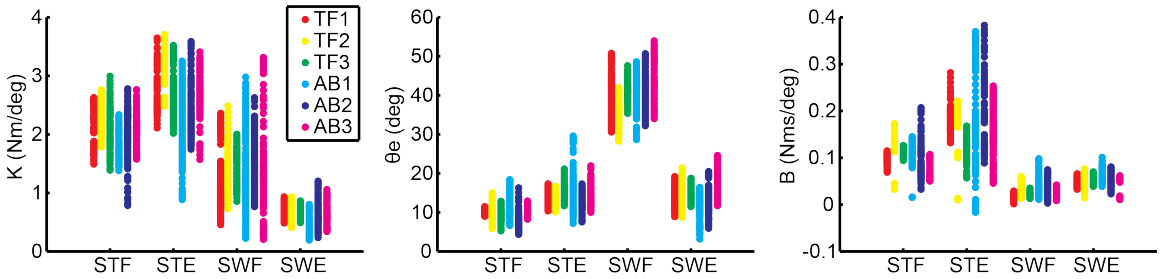

Fig. 2. Range of impedance parameters for each subject explored by reinforcement learning.

$$I_{sB} = \int_{IDS} F_{sy}dt + \int_{SS-} F_{sy}dt,$$
$$I_{sP} = \int_{TDS} F_{sy}dt + \int_{SS+} F_{sy}dt, \quad (11)$$

where s is the side indicator of each leg, where p indicates prosthetic side and i indicates intact side. B denotes braking impulse, P denotes propulsive impulse, and F_sy is the antero-posterior ground reaction force from corresponding limb.

We calculated the braking symmetry index (SI) and propulsion symmetry index (SI) between the prosthetic side and the intact side, which was respectively equivalent to the contribution of impulse from each leg.

$$SI_B = \frac{I_{iB} - I_{pB}}{1/2(I_{iB} + I_{pB})}$$
$$SI_P = \frac{I_{iP} - I_{pP}}{1/2(I_{iP} + I_{pP})} \quad (12)$$

In addition, the net inter-limb impulse was calculated by adding the braking impulse of the prosthetic limb (leading limb) and the propulsive impulse of the intact limb (trailing limb): $I_{iP} + I_{pB}$.

E. Data exclusion criteria

We excluded data in the following cases: 1) a subject tripped during walking, i.e., the vertical ground reaction force during the swing phase was greater than $80N$, 2) the feature extraction procedure failed to detect stance flexion and/or stance extension, 3) the number of gait cycles was less than 4, i.e., insufficient gait cycles for the auto-tuner to compute an new impedance parameter update, and 4) the swing flexion angle was less than 45 degrees. The above criteria ensured fairness and completeness of the data to ensure the RL-based auto-tuner functioned under reasonable conditions for the control of the wearer-prosthesis system.

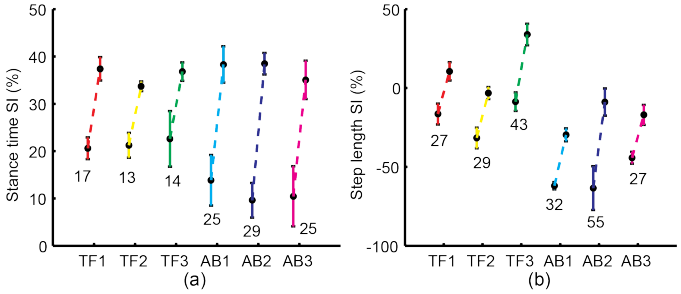

Fig. 3. Stance time SI and step length SI changed significantly during the control parameter exploration for all six subjects. The mean and standard deviation of the iterations with maximum and minimum values are compared. A paired t-test revealled significant difference for all measurements ($p < 0.01$). a) and b) The temporal-spatial gait symmetry indexes covered a wide range relative to variances without control change (3% for stance time SI, 5% for step length SI). No subject could generate perfect stance time symmetry, but some could generate perfect step length symmetry.

F. Statistical analysis

A one-way ANOVA was conducted to compare the effect of the different control/mechanics of the robotic knee prosthesis on the prosthetic knee kinematics, temporal-spatial gait symmetry, and AP impulses, with significance set at $p < 0.01$. Pearson correlation coefficient analysis was used to evaluate the relationship between the inter-limb impulse measurements (propulsion SI, braking SI, and net inter-limb impulse) and the gait symmetry measurements (i.e., stance time SI, and step length SI), with significance set at $p < 0.01$. All statistics were conducted using MATLAB (MathWorks, Natick, MA).

III. RESULTS

A. Changes in prosthetic knee kinematics, temporal-spatial symmetry indices, and bilateral AP impulses caused by changes in prosthesis control/mechanics

The RL-based prosthesis tuning procedure resulted in testing an average of 155 ($\pm$10) different combinations of the 12-dimensional control parameters (Fig. 2), which determined

the mechanics of the robotic knee prosthesis, on each subject. RL induced changes in prosthesis control parameters led to changes in prosthesis knee kinematics, bilateral AP impulses, and temporal-spatial gait symmetry.

1) The control parameters (mechanics) of the robotic knee prosthesis influenced the prosthetic knee kinematics significantly ($p < 0.01$). They elicited wide ranges of responses in peak stance flexion angle, peak stance extension angle, peak swing flexion angle, and peak swing extension angle. Averaged across human subjects, the respective ranges were 12.5 degrees, 15.6 degrees, 11.3 degrees and 14.8 degrees. The average standard deviation of the peak angles when using the same control parameters was 1.2 degrees across all tested control settings and subjects. The angle variations caused by parameter changes were significantly larger than those due to the intrinsic variation of human walking with fixed prosthesis control ($p < 0.01$).

2) A change in the robotic knee prosthesis control elicited a change in the braking impulse and propulsive impulse on both lower limbs. The braking impulse and propulsive impulse of the prosthetic limb changed in the range of 1.95 $\%BW \cdot s$ and 1.73 $\%BW \cdot s$, respectively. The braking impulse and propulsive impulse of the intact limb changed in the range of 2.42 $\%BW \cdot s$ and 1.85 $\%BW \cdot s$, respectively. The average standard deviation of the impulse measurements was 0.35 $\%BW \cdot s$ across all control settings and subjects. Note that the positive impulse was aligned with the walking direction. There was a significant effect of prosthetic knee control/mechanics on impulses at the 0.01 level for all subjects.

3) Similarly, changes in the prosthesis control led to significantly greater variations in stance time symmetry and step length symmetry than the variations of amputees walking with a fixed prosthesis control. Measuring within each set of control parameter, the average standard deviations of stance time SI and step length SI across human subjects and different control parameters were 3.3% and 5.7%, respectively. Compared to these values, changes of the prosthesis control led to a much greater variation of gait symmetry in stance time and step length (Fig. 3). An analysis of variance showed that the effects of prosthetic knee control/mechanics on stance time SI and step length SI were statistically significant ($p < 0.01$).

B. Correlation between inter-limb impulse measurements and temporal-spatial symmetry indices

As shown in Table II, the propulsion SI and braking SI were correlated with stance time SI, but they were not consistent across subjects. Instead, the net inter-limb impulse was consistently and significantly correlated with the stance time SI across all subjects ($p < 0.01$) and yielded the highest correlation coefficient ($R = 0.7 \pm 0.08$). Fig. 4 shows amputees' data as an example. The stance time SI decreased, indicating improved stance time symmetry, with decreased net inter-limb impulse.

Both propulsion SI and braking SI were consistently and significantly correlated with the step length SI for all subjects (Table II). This observation was consistent with previous studies on stroke patients [27], [46]. The net inter-limb impulse was not consistently correlated with step length SI across subjects. The positive step length SI indicated a longer intact side step length, measured by the anteroposterior distance between two calcaneus markers at intact side heel strike.

Upon further examination of the kinetic coordination between prosthetic limb and intact limb, we found that the cause of gait temporal asymmetry varies across subjects. Using the results derived from TF2 and TF3 as examples, TF2 generated symmetrical braking impulse, but showed asymmetrical propulsion with weak propulsive impulse from the prosthetic limb (Fig. 5(a)). TF3, on the other hand, generated symmetrical propulsion impulse, but showed asymmetrical braking impulse with lower braking impulse from the prosthetic limb (Fig. 5(b)). Both cases resulted in temporal asymmetry. In addition, the change of impulse SI resulted from opposite impulse changes from both limbs, i.e., increased braking/propulsive impulse from prosthetic side accompanied by decreased braking/propulsive impulse from intact side (Fig. 5(a) and Fig. 5(b)).

C. Prosthetic knee kinematics with best stance time SI

We also checked the knee kinematics of subjects at their best stance time SI (Fig. 6). Although the kinematics varied across subjects, it demonstrated that the stance flexion from the robotic knee prosthesis at the loading response seems to be necessary for wearer-prosthesis system to exhibit the best stance time symmetry observed in this study.

IV. Conclusion and discussion

Optimizing wearable robots to maximize each individual wearer's biomechanical performance is an emerging and important research topic in the field. Our research contributes to the important knowledge of wearer-prosthesis interaction. Although optimizing exoskeleton control has been reported to minimize the metabolic cost of able-bodied wearers in walking [38], [39], optimizing prosthesis mechanics to maximize human gait performance has not been demonstrated because it is unclear whether and how prosthesis mechanics influences the human's overall gait, balance, and energy expenditure. To fill this knowledge gap, in this study we investigated the effects of complex robotic knee prosthesis control, consisting of 12 control parameters, on gait temporal-spatial SI and inter-limb AP impulses. Enabled by a novel application of the RL-based prosthesis tuning, which allows for exploration of different control parameter combinations with the human in the loop, we found that the wearer's gait temporal-spatial SI was sensitive to the mechanics of prosthetic knee. Adjusting prosthesis mechanics alone elicited changes in stance time and step length on both limbs; the bilateral changes were generally in an opposite direction, which led to significant variations in the symmetry indices (Fig. 5). The observed modification of motion in the human's intact limb was likely caused passively or involuntarily since we neither instructed the subjects to alter their gait voluntarily nor informed them when the prosthesis control was adjusted. Appropriate prosthesis control could yield step length symmetry in some subjects, though none of the prosthesis controls tested on our subjects led to stance

TABLE II
CORRELATION ANALYSIS BETWEEN IMPULSE MEASUREMENTS AND GAIT SYMMETRY

R	Stance Time SI (%)						Step length SI (%)					
	TF1	TF2	TF3	AB1	AB2	AB3	TF1	TF2	TF3	AB1	AB2	AB3
Propulsion SI (%)	0.03	0.07	**0.33**	**0.79**	**0.45**	**0.74**	**-0.65**	**-0.56**	**-0.48**	**-0.60**	**-0.82**	**-0.52**
Braking SI(%)	**0.44**	**0.56**	**0.38**	0.16	-0.03	-0.10	**0.82**	**0.77**	**0.67**	**0.47**	**0.79**	**0.56**
Net inter-limb impulse (I)	**-0.76**	**-0.75**	**-0.58**	**-0.79**	**-0.59**	**-0.75**	**-0.51**	-0.18	**-0.60**	0.03	**-0.32**	0.00
Net inter-limb impulse (P)	**0.79**	**0.71**	**0.62**	**0.79**	**0.62**	**0.65**	**0.52**	0.17	**0.54**	-0.06	**0.26**	0.05

Bold indicating $p < 0.01$.

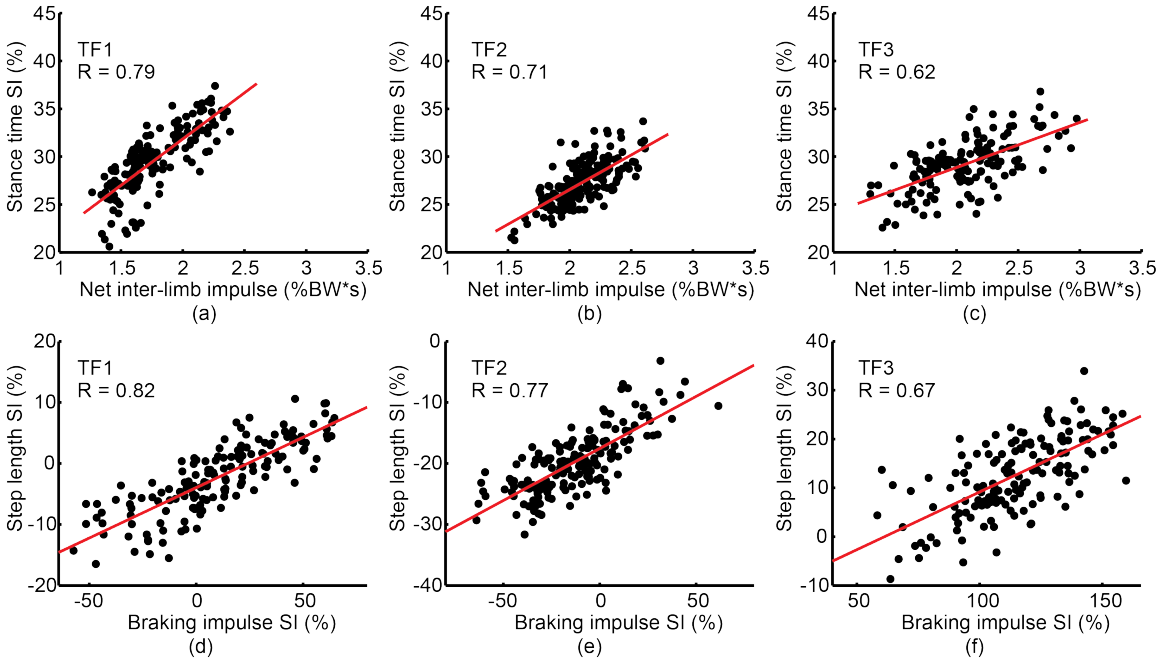

Fig. 4. Correlations between impulse measurements and gait symmetry from TF subjects. (a)-(c) Correlation between net inter-limb impulse (normalized to body weight) and the stance time SI. (d)-(f) Correlation between braking impulse SI and step length SI. The net inter-limb impulse was the net impulse (summation of propulsive impulse of the intact limb and braking impulse of the prosthetic limb) during the transition from intact limb to prosthetic limb. A red line is the least squares fit to the data.

time symmetry (Fig. 3). These results indicated that optimizing prosthesis control to improve temporal-spatial symmetry is possible, although adjusting prosthesis control alone seems to be limited to maximize normative gait temporal-spatial symmetry. A previous study demonstrated that human active adaptation could also improve gait symmetry even with fixed control/mechanics of the robotic knee prosthesis [47]. Thus, it might be necessary to combine rehabilitation training and prosthesis optimization to further improve the gait symmetry in the wearer-prosthesis system.

Directly using the 12 prosthesis control parameters to explain gait temporal-spatial symmetry is inadequate as the symmetry measurements also involve motor behavior of the intact limb, which varies greatly across humans. Instead, we examined propulsive and braking AP impulses of both the prosthetic limb and the intact limb because AP impulses in walking are the results of interactions between both lower limbs and the environment. Furthermore, these impulses have previously explained gait characteristics, such as temporal-spatial symmetry [27], [32] and walking speed [48]. In addition, the propulsive and braking impulses on the prosthetic

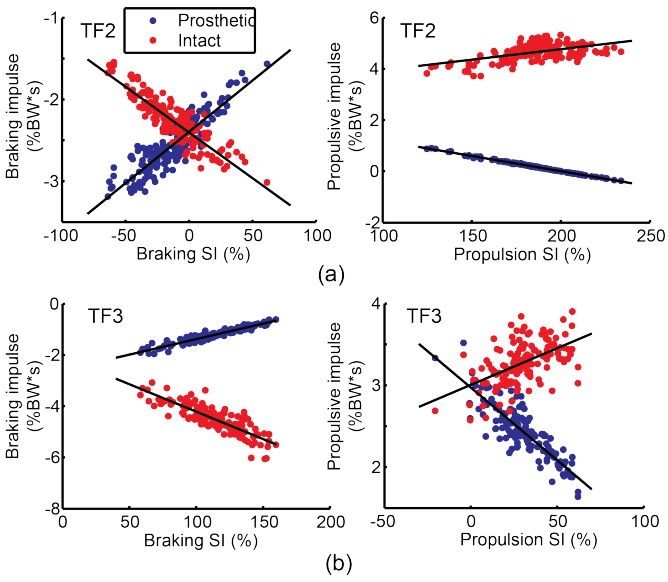

Fig. 5. Propulsive impulse and braking impulse of two TF subjects as examples.

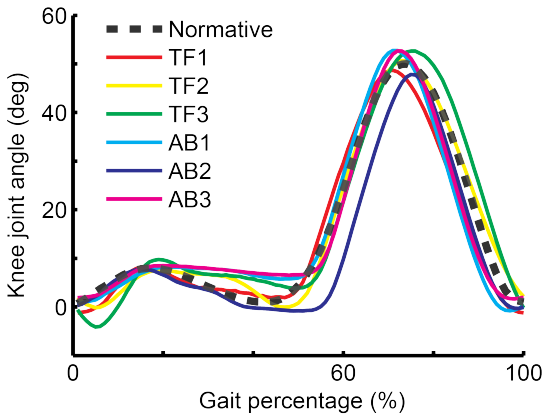

Fig. 6. The knee kinematics of all subjects at their best stance time SI. Each of knee kinematics as averaged across a few control parameter conditions whose stance time SI lies in the top 5 among all (∼500) control parameter conditions.

side are directly related to the prosthesis control. Our study showed that the net inter-limb impulse, which reflects coordinated propulsive and breaking impulses between the intact and prosthetic limbs during limb transition, were associated with temporal asymmetry (Table. II). Balancing the leading limb braking impulse and trailing limb propulsion improved temporal symmetry. This observation was consistently observed across all subjects in this study and can be explained biomechanically. During transition from the mid-stance of one limb to the mid-stance of the other, the net inter-limb impulse is proportional to the change of forward velocity of center of mass. If the net AP inter-limb impulse is balanced to zero, the center of mass velocities of each limb are the same (i.e., symmetrical) at mid-stance. Otherwise, unbalanced net AP inter-limb impulse accelerates or decelerates the center of mass, causing one side of the limbs to produce shorter or longer stance time on that limb [27]. Interestingly, almost all previous studies have mainly attributed the gait asymmetry in lower limb amputees to an insufficient propulsive force or impulse from the prosthetic limb [27], while our study showed that insufficient braking in the prosthesis limb could also elicit temporal gait asymmetry. For example, TF2 had insufficient propulsive impulse while TF3 had insufficient braking impulse; both generated asymmetrical stance time in walking. Moreover, our study showed that the SI of the propulsive or braking impulse was associated with the step length SI, which is consistent with previous findings on pathologic gait [32]. Therefore, it is critical to understand the cause of gait asymmetry for each individual in order to produce optimal prosthesis control and/or guide rehabilitation to improve gait symmetry.

In addition to our major findings on the relationship between symmetry and impulses, our results (Fig. 6) may also shed light on a long-standing question in the field of prostheses: is stance flexion necessary for a prosthetic knee? In able-bodied humans, the knee joint generates small flexion during early stance (i.e., loading response period), which serves two functions: shock absorption and hip height maintenance [49]. However, many previous studies on powered knee prostheses ignored stance flexion [50], [51] due to the wearer's preference. This was because the wearers might have already adapted to their previous daily passive devices, which usually locked the knee joint to a full extension for weight support during stance. In addition, some wearers reported a sense of instability when the prosthesis knee flexed during stance [52]. In our study, training of the subjects helped them to become confident and comfortable with the prosthesis knee stance flexion in walking. More importantly, we noted knee stance flexion during early stance across all subjects from those tests that rendered the best stance time symmetry (Fig. 6). Since shock absorption after foot contact is pertinent to breaking impulse, the observation further confirmed the importance of prosthesis knee control in early stance. Generating knee stance flexion with eccentric torque in early stance might be necessary for prosthesis control to improve gait symmetry. However, there is no clear relationship between the prosthesis features and the gait symmetry index, and the target knee kinematics in this study cannot guarantee the best stance time symmetry for each participant. Hence, personalizing the target knee features may be necessary in order to minimize gait asymmetry.

Our research method based on reinforcement learning may transform the study of physical wearer-robot interaction. Advanced wearable machines, such as neuroprostheses, robotic prostheses, and exoskeletons, typically involve high-dimensional control parameters that need to be tuned for personalized gait assistance. In order to study the influence of wearable machines on the human's physical performance, two methods are usually adopted: computer simulation and empirical study. Computer simulation allows for a systematic investigation of wearable machine controls with high-dimensionality, but it often ignores or simplifies the human neural reactions and pathological conditions, leading to conclusions that do not match experimental observations [53]. The empirical approach allows study of the wearer-robot system directly, but it is extremely difficult, if possible, to investigate more than 3 parameters at a time. To address this challenge, we introduced a novel application of a powerful RL-based prosthesis tuning system. The RL-based prosthetic control enabled the human wearers to walk safely via safety constraints, and generated variant control parameter settings that yielded significant changes in the wearer-prosthesis system, including ground reaction force/impulse and temporal-spatial symmetry. With the flexible neural network structure, this RL-based control framework can be extended to exoskeletons and other complex, wearable assistive devices to potentially benefit patient populations other than lower limb amputees. More work is needed to validate the generalizability of this framework with different controllers for different wearable devices and the effectiveness of this framework through comparison with other exploration methods.

Finally, the nature of our research has a limiting effect on the number of subjects. We included three able-bodied subjects in this study because able-bodied subjects could reveal the control performance of prosthesis and had been recruited in wearer-prosthesis studies [20], [34]. Despite the inter-human variation, all subjects yielded consistent and statistic

significant correlation between the net inter-limb impulse and the stance time SI, as well as between propulsion/braking impulse SI and step length SI. Another limitation is that the evaluation criteria were designed for immediately changed performance measurements (e.g., knee kinematics). To study slow responding measurements (e.g., metabolic cost), this method will need more time to get reliable and representative performance. Additionally, this study limited its scope to gait performance measurements by temporal-spatial symmetry, and to treadmill walking test condition. It would be interesting as future work to 1) use RL-based control to understand the influence of prosthesis mechanics on other gait metrics (e.g., stability, intact joint loading, or human cognitive responses) in a realistic context (e.g., level-ground walking with varied speed), and 2) utilize the propulsion and braking impulse observations as feedback to personalize the control parameters so as to improve gait symmetry.

ACKNOWLEDGMENT

The authors would like to thank Dr. M. Liu and Dr. S. Huang for their valuable input of data analysis; prosthetist D. Frankena and physical therapist M. Soyars for prosthesis fitting and subject training, and all the participants for their time and efforts.

REFERENCES

[1] F. Sup, H. A. Varol, J. Mitchell, T. J. Withrow, and M. Goldfarb, "Preliminary evaluations of a self-contained anthropomorphic transfemoral prosthesis," *IEEE/ASME Transactions on Mechatronics*, vol. 14, no. 6, pp. 667–676, Dec. 2009.

[2] E. C. Martinez-Villalpando and H. Herr, "Agonist-antagonist active knee prosthesis: a preliminary study in level-ground walking," *Journal of Rehabilitation Research and Development*, vol. 46, no. 3, pp. 361–373, May 2009.

[3] L. Ambrozic, M. Gorsic, J. Geeroms *et al.*, "CYBERLEGs: A user-oriented robotic transfemoral prosthesis with whole-body awareness control," *IEEE Robotics and Automation Magazine*, vol. 21, no. 4, pp. 82–93, Dec. 2014.

[4] T. Lenzi, M. Cempini, L. J. Hargrove, and T. A. Kuiken, "Design, development, and testing of a lightweight hybrid robotic knee prosthesis," *The International Journal of Robotics Research*, vol. 37, no. 8, pp. 953–976, Jul. 2018.

[5] E. J. Rouse, L. M. Mooney, and H. Herr, "Clutchable series-elastic actuator: Implications for prosthetic knee design," *The International Journal of Robotics Research*, vol. 33, no. 13, pp. 1611–1625, Oct. 2014.

[6] C. D. Hoover, G. D. Fulk, and K. B. Fite, "Stair ascent with a powered transfemoral prosthesis under direct myoelectric control," *IEEE/ASME Transactions on Mechatronics*, vol. 18, no. 3, pp. 1191–1200, 2013.

[7] R. D. Gregg and J. W. Sensinger, "Towards biomimetic virtual constraint control of a powered prosthetic leg," *IEEE Transactions on Control Systems Technology*, vol. 22, no. 1, pp. 246–254, Jan. 2014.

[8] H. Huang, T. a. Kuiken, and R. D. Lipschutz, "A strategy for identifying locomotion modes using surface electromyography," *IEEE Transactions on Biomedical Engineering*, vol. 56, no. 1, pp. 65–73, Jan. 2009.

[9] He Huang, Fan Zhang, L. J. Hargrove, Zhi Dou, D. R. Rogers, and K. B. Englehart, "Continuous Locomotion-Mode Identification for Prosthetic Legs Based on Neuromuscular-Mechanical Fusion," *IEEE Transactions on Biomedical Engineering*, vol. 58, no. 10, pp. 2867–2875, Oct. 2011.

[10] L. J. Hargrove, A. J. Young, A. M. Simon *et al.*, "Intuitive control of a powered prosthetic leg during ambulation: A randomized clinical trial," *JAMA - Journal of the American Medical Association*, vol. 313, no. 22, pp. 2244–2252, 2015.

[11] B. E. Lawson, H. A. Varol, A. Huff, E. Erdemir, and M. Goldfarb, "Control of stair ascent and descent with a powered transfemoral prosthesis," *IEEE Transactions on Neural Systems and Rehabilitation Engineering*, vol. 21, no. 3, pp. 466–473, May 2013.

[12] F. Zhang and H. Huang, "Source selection for real-time user intent recognition toward volitional control of artificial legs," *IEEE Journal of Biomedical and Health Informatics*, vol. 17, no. 5, pp. 907–914, 2013.

[13] E. D. Ledoux and M. Goldfarb, "Control and Evaluation of a Powered Transfemoral Prosthesis for Stair Ascent," *IEEE Transactions on Neural Systems and Rehabilitation Engineering*, vol. 25, no. 7, pp. 917–924, Jul. 2017.

[14] C. Jayaraman, S. Hoppe-Ludwig, S. Deems-Dluhy *et al.*, "Impact of powered knee-ankle prosthesis on low back muscle mechanics in transfemoral amputees: A case series," *Frontiers in Neuroscience*, vol. 12, no. MAR, 2018.

[15] S. Rezazadeh, D. J. Lambert, D. Quintero, R. D. Gregg, E. Reznick, and L. Gray, "Intuitive Clinician Control Interface for a Powered Knee-Ankle Prosthesis: A Case Study," *IEEE Journal of Translational Engineering in Health and Medicine*, vol. 6, no. December, pp. 1–9, 2018.

[16] S. Rezazadeh, D. Quintero, N. Divekar, E. Reznick, L. Gray, and R. D. Gregg, "A Phase Variable Approach for Improved Rhythmic and Non-Rhythmic Control of a Powered Knee-Ankle Prosthesis," *IEEE Access*, vol. 7, pp. 109 840–109 855, 2019.

[17] A. M. Simon, K. a. Ingraham, N. P. Fey *et al.*, "Configuring a powered knee and ankle prosthesis for transfemoral amputees within five specific ambulation modes," *PLoS ONE*, vol. 9, no. 6, p. e99387, Jun. 2014.

[18] Y. Wen, J. Si, A. Brandt, X. Gao, and H. Huang, "Online Reinforcement Learning Control for the Personalization of a Robotic Knee Prosthesis," *IEEE Transactions on Cybernetics*, vol. PP, pp. 1–11, 2019.

[19] H. Huang, D. L. Crouch, M. Liu, G. S. Sawicki, and D. Wang, "A Cyber Expert System for Auto-Tuning Powered Prosthesis Impedance Control Parameters," *Annals of Biomedical Engineering*, vol. 44, no. 5, pp. 1613–1624, Sep. 2016.

[20] P. Malcolm, R. E. Quesada, J. M. Caputo, and S. H. Collins, "The influence of push-off timing in a robotic ankle-foot prosthesis on the energetics and mechanics of walking," *Journal of NeuroEngineering and Rehabilitation*, vol. 12, no. 1, p. 14, 2015.

[21] R. E. Quesada, J. M. Caputo, and S. H. Collins, "Increasing ankle push-off work with a powered prosthesis does not necessarily reduce metabolic rate for transtibial amputees," *Journal of Biomechanics*, vol. 49, no. 14, pp. 3452–3459, 2016.

[22] J. Realmuto, G. Klute, and S. Devasia, "Preliminary Investigation of Symmetry Learning Control for Powered Ankle-Foot Prostheses," *2019 Wearable Robotics Association Conference, WearRAcon 2019*, pp. 40–45, 2019.

[23] M. Liu, F. Zhang, P. Datseris, and H. Huang, "Improving Finite State Impedance Control of Active-Transfemoral Prosthesis Using Dempster-Shafer Based State Transition Rules," *Journal of Intelligent & Robotic Systems*, vol. 76, no. 3, pp. 461–474, Dec. 2014.

[24] Y. Sagawa, K. Turcot, S. Armand, A. Thevenon, N. Vuillerme, and E. Watelain, "Biomechanics and physiological parameters during gait in lower-limb amputees: A systematic review," *Gait and Posture*, vol. 33, no. 4, pp. 511–526, Feb. 2011.

[25] S. a. Gard, "Use of Quantitative Gait Analysis for the Evaluation of Prosthetic Walking Performance," *Journal of Prosthetics and Orthotics*, vol. 18, no. 6, pp. P93–P104, 2006.

[26] A. L. Hof, R. M. van Bockel, T. Schoppen, and K. Postema, "Control of lateral balance in walking: Experimental findings in normal subjects and above-knee amputees," *Gait and Posture*, vol. 25, no. 2, pp. 250–258, 2007.

[27] P. G. Adamczyk and A. D. Kuo, "Mechanisms of Gait Asymmetry Due to Push-Off Deficiency in Unilateral Amputees," *IEEE Transactions on Neural Systems and Rehabilitation Engineering*, vol. 23, no. 5, pp. 776–785, Sep. 2015.

[28] M. Schaarschmidt, S. W. Lipfert, C. Meier-Gratz, H. C. Scholle, and A. Seyfarth, "Functional gait asymmetry of unilateral transfemoral amputees," *Human Movement Science*, vol. 31, no. 4, pp. 907–917, 2012.

[29] H. L. Jarvis, A. N. Bennett, M. Twiste, R. D. Phillip, J. Etherington, and R. Baker, "Temporal Spatial and Metabolic Measures of Walking in Highly Functional Individuals With Lower Limb Amputations," *Archives of Physical Medicine and Rehabilitation*, vol. 98, no. 7, pp. 1389–1399, 2017.

[30] R. Gailey, "Review of secondary physical conditions associated with lower-limb amputation and long-term prosthesis use," *Journal of Rehabilitation Research and Development*, vol. 45, no. 1, pp. 15–30, 2008.

[31] D. M. Ehde, D. G. Smith, J. M. Czerniecki, K. M. Campbell, D. M. Malchow, and L. R. Robinson, "Back pain as a secondary disability in persons with lower limb amputations," *Archives of Physical Medicine and Rehabilitation*, vol. 82, no. 6, pp. 731–734, 2001.

[32] C. K. Balasubramanian, M. G. Bowden, R. R. Neptune, and S. A. Kautz, "Relationship Between Step Length Asymmetry and Walking Perfor-

mance in Subjects With Chronic Hemiparesis," *Archives of Physical Medicine and Rehabilitation*, vol. 88, no. 1, pp. 43–49, 2007.

[33] J. R. Perttunen, E. Anttila, J. Södergård, J. Merikanto, and P. V. Komi, "Gait asymmetry in patients with limb length discrepancy," *Scandinavian Journal of Medicine and Science in Sports*, vol. 14, no. 1, pp. 49–56, 2004.

[34] F. Sup, A. Bohara, and M. Goldfarb, "Design and Control of a Powered Transfemoral Prosthesis," *The International Journal of Robotics Research*, vol. 27, no. 2, pp. 263–273, Feb. 2008.

[35] Y. Wen, A. Brandt, M. Liu, H. Huang, and J. Si, "Comparing Parallel and Sequential Control Parameter Tuning for a Powered Knee Prosthesis," in *IEEE International Conference on Systems, Man, and Cybernetics*, Banff, Canada, 2017, pp. 1716–1721.

[36] J. Si and Y.-t. Wang, "On-Line Learning Control by Association and Reinforcement," *IEEE Transactions on Neural Networks*, vol. 12, no. 2, pp. 264–276, Mar. 2001.

[37] J. Si, A. G. Barto, W. B. Powell, and D. Wunsch, *Handbook of learning and approximate dynamic programming*. New Jersey: John Wiley & Sons, 2004.

[38] J. Zhang, P. Fiers, K. A. Witte *et al.*, "Human-in-the-loop optimization of exoskeleton assistance during walking," *Science*, vol. 356, no. 6344, pp. 1280–1284, Jun. 2017.

[39] Y. Ding, M. Kim, S. Kuindersma, and C. J. Walsh, "Human-in-the-loop optimization of hip assistance with a soft exosuit during walking," *Science Robotics*, vol. 3, no. 15, p. eaar5438, Feb. 2018.

[40] Y. Wen, J. Si, X. Gao, S. Huang, and H. Huang, "A New Powered Lower Limb Prosthesis Control Framework Based on Adaptive Dynamic Programming," *IEEE Transactions on Neural Networks and Learning Systems*, vol. 28, no. 9, pp. 2215–2220, Sep. 2017.

[41] R. Enns and J. Si, "Apache Helicopter Stabilization Using Neural Dynamic Programming," *Journal of Guidance, Control, and Dynamics*, vol. 25, no. 1, pp. 19–25, Jan. 2002.

[42] R. Enns and J. Si, "Helicopter Trimming and Tracking Control Using Direct Neural Dynamic Programming," *IEEE Transactions on Neural Networks*, vol. 14, no. 4, pp. 929–939, Jul. 2003.

[43] R. Enns and J. Si, "Helicopter flight-control reconfiguration for main rotor actuator failures," *Journal of guidance, control, and dynamics*, vol. 26, no. 4, pp. 572–584, Jul. 2003.

[44] C. Lu, J. Si, and X. Xie, "Direct Heuristic Dynamic Programming for Damping Oscillations in a Large Power System," *IEEE Transactions on Systems, Man, and Cybernetics, Part B: Cybernetics*, vol. 38, no. 4, pp. 1008–1013, Aug. 2008.

[45] M. G. Bowden, C. K. Balasubramanian, R. R. Neptune, and S. A. Kautz, "Anterior-posterior ground reaction forces as a measure of paretic leg contribution in hemiparetic walking," *Stroke*, vol. 37, no. 3, pp. 872–876, 2006.

[46] J. L. Allen, S. A. Kautz, and R. R. Neptune, "Step length asymmetry is representative of compensatory mechanisms used in post-stroke hemiparetic walking," *Gait and Posture*, vol. 33, no. 4, pp. 538–543, 2011.

[47] A. Brandt, W. Riddick, J. Stallrich, M. Lewek, and H. Huang, "Effects of extended powered knee prosthesis stance time via visual feedback on gait symmetry of individuals with unilateral amputation: a preliminary study," *Journal of NeuroEngineering and Rehabilitation*, vol. 16, no. 1, pp. 1–12, 2019.

[48] C. L. Peterson, S. A. Kautz, and R. R. Neptune, "Braking and propulsive impulses increase with speed during accelerated and decelerated walking," *Gait and Posture*, vol. 33, no. 4, pp. 562–567, 2011.

[49] M. W. Whittle, *Gait analysis: an introduction*, fourth edi ed., M. W. Whittle, Ed. Heidi Harrison, 2002, vol. 3.

[50] T. Lenzi, L. J. Hargrove, and J. Sensinger, "Speed-adaptation mechanism: Robotic prostheses can actively regulate joint torque," *IEEE Robotics and Automation Magazine*, vol. 21, no. 4, pp. 94–107, Dec. 2014.

[51] H. Vallery, R. Burgkart, C. Hartmann, J. Mitternacht, R. Riener, and M. Buss, "Complementary limb motion estimation for the control of active knee prostheses," *Biomedizinische Technik*, vol. 56, no. 1, pp. 45–51, 2011.

[52] F. Zhang, M. Liu, and H. Huang, "Effects of locomotion mode recognition errors on volitional control of powered above-knee prostheses," *IEEE Transactions on Neural Systems and Rehabilitation Engineering*, vol. 23, no. 1, pp. 1128–1131, Jan. 2015.

[53] M. L. Handford and M. Srinivasan, "Robotic lower limb prosthesis design through simultaneous computer optimizations of human and prosthesis costs," *Scientific Reports*, no. 19983, pp. 1–7, Feb. 2016.